

ARTICLE

Adsorbate-induced demagnetization: borohydride on magnetic substrates

Ryan Lacdao Arevalo^{*,1}, Mary Clare Sison Escaño²,
Allan Abraham Bustria Padama³, and Hideaki Kasai^{4,5,6}

¹Faculty of Science, Technology and Mathematics, Philippine Normal University,
Taft Avenue, Manila 1000, Philippines

²Graduate School of Engineering, University of Fukui, 3-9-1 Bunkyo, Fukui 910-8507, Japan

³Institute of Mathematical Sciences and Physics, College of Arts and Sciences,
University of the Philippines Los Baños, Los Baños, Laguna 4031, Philippines

⁴National Institute of Technology, Akashi, Hyogo 674-8501, Japan

⁵Institute of Industrial Science, The University of Tokyo, Meguro, Tokyo 153-8505, Japan

⁶Graduate School of Engineering, Osaka University, Suita, Osaka 565-0871, Japan

Abstract—Elucidating the effect of different adsorbates on the magnetic properties of substrates has found useful applications in the design of magnetic devices. In this paper, we show through first principles calculations that the adsorption of borohydride on magnetic substrates (pure 3d or first row transition metals such as Cr, Mn, Fe, Co, and Ni and Au-3d metal alloys) induces the demagnetization of the substrate atoms that directly bind with borohydride. We note a forward shifting of the spin-up and backward shifting of the spin-down components of the metal d band, before and after the adsorption of borohydride, demagnetizing the substrate. The inclusion of spin-polarization in the calculation affects the adsorption energy of borohydride but not its adsorption structure and relative energies on different substrates. Large substrate demagnetization is noted for substrates that promote the strong adsorption of borohydride.

Keywords—demagnetization, density functional theory, gold alloys, magnetization, catalysis, computational physics

INTRODUCTION

The effect of molecule or atom adsorption on the magnetic properties of substrates has been widely studied over the past years, motivated by their profound potential in the atomic-scale design of magnetic devices, in Spintronics, and other useful applications as catalytic and multifunctional magneto-optic materials [1-5]. Recently, we have reported that the adsorption of borohydride on surfaces induces the demagnetization of the metal substrates [6-7]. Such studies on the interaction of borohydride on metal surfaces find their application in the design of catalysts for hydrogen generation systems and direct borohydride fuel cells [8-10].

In this paper, we report the effect of borohydride adsorption on the magnetic properties of pure and alloyed metal substrates. Using pure 3d (first row) transition metals (Cr, Mn, Fe, Co, and Ni) and their alloys with Au as substrates (Au-3d alloys), we analyzed the demagnetization of the substrates in relation to structure and stability of borohydride.

COMPUTATIONAL MODEL

The initial adsorption of borohydride anion (BH_4^-) on catalysts is accompanied by a simultaneous transfer of electron generating $BH_y^* + (4-y)H^*$ (with $y = 1, 2, 3$ for dissociative and $y = 4$ for molecular adsorption). Here, the asterisk (*) denotes surface bound species. In our simulation, the adsorbed species BH_y^* was modeled in an overall neutral unit cell. This model was also utilized in other related DFT studies on borohydride and for oxidative adsorption of other anions like BF_4^- [11] and OH^- [12-13]. The stable configuration of adsorbed borohydride was determined by exhausting a number of possible orientations on one side of the slab. This includes the H-up and H-down orientations (Fig. 1) of the tetragonal borohydride with B at the high symmetry sites on the surface (top, bridge, hcp hollow and fcc hollow sites) and in-plane rotation. The adsorption energy, E_{ads} , on each metal was computed by taking the difference between the total energy of the borohydride-slab system in the lowest energy adsorption site and the summed energies of the relaxed clean surface and gas-phase borohydride.

The 3d transition metal substrates (Cr, Mn, Fe, Co, and Ni) were modeled using four-layer slabs in a (3×3) unit cell making $\sim 1/9$ ML of adsorbate coverage. Structural optimization required

*Corresponding Author
Email Address: arevalo.rl@pnu.edu.ph
Submitted: August 13, 2015
Revised: N/A
Accepted: June 6, 2016
Published: August 11, 2016

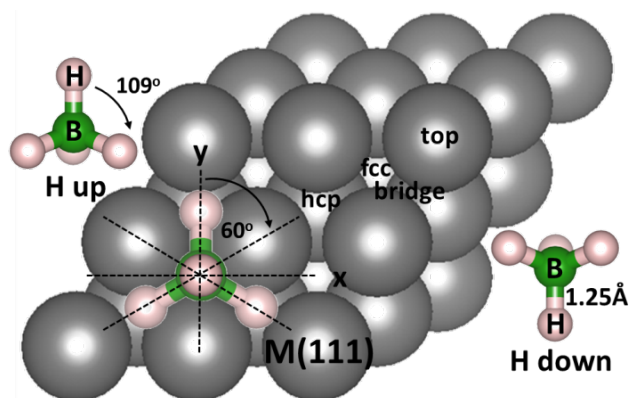


Fig. 1. The stable configuration of adsorbed borohydride (BH_4^*) was determined by initially placing the tetrahedral borohydride in H-up and H-down orientations with B at the high symmetry sites on the surface (top, bridge, hcp hollow and fcc hollow sites) and rotating the molecule on the xy plane.

the adsorbate and the top two layers of the slab to fully relax in all directions while the bottom two layers of the slab fixed at their bulk structure. The fcc (111) facet of these metals was used to rule out the structural differences between different surfaces and to extract meaningful trends in properties as a function of substrate identity. This is certainly realistic for Ni and Cu since they occur naturally as fcc metals. For Cr, Mn, Co, and Fe, these fcc phases are important when considering epitaxial growth on substrates such as copper [14]. The calculated lattice constants for Cr, Mn, Fe, Co, and Ni are respectively: 3.61 Å, 3.50 Å, 3.45 Å, 3.45 Å, and 3.53 Å, in excellent agreement with those reported in the literatures (Cr: 3.62 Å [15], Mn: 3.30 Å to 3.57 Å [16], Fe: 3.60 Å [17], Co: 3.31 Å to 3.51 Å [16], Ni: 3.52 Å [18]). Each slab is separated by ~ 15.0 Å of vacuum, which is large enough to avoid the surface atom interaction along z axis with the neighboring unit cells. Electric dipole correction layer in the vacuum area was used to cut the dipole interactions between the repeated image layer systems. Optimization is terminated when the Hellman-Feynman forces acting on each atom dropped below 0.005 eV/Å.

Spin polarized density functional theory (DFT) calculations were implemented via the Vienna ab initio simulation package (VASP) [19-22]. The interaction between ions and electrons were described using projector augmented wave (PAW) method [23-24]. Plane wave basis sets were employed with energy cut-off of 400 eV. The exchange-correlation term was described using generalized gradient approximation (GGA) based on Perdew-Burke-Ernzerhof (PBE) functional [25-26]. The surface Brillouin zone integrations were performed on a grid of (4x4x1) Monkhorst-Pack k-points [27] using Methfessel-Paxton

smearing [28] of $\sigma = 0.2$ eV. Conjugate-gradient algorithm [29] was used to relax the ions into their ground state. Convergence of numerical results with respect to the slab thickness, the kinetic energy cut-off and the k-point was established.

RESULTS AND DISCUSSION

Adsorption on pure 3d metal substrates

We first discuss the structure of borohydride which was determined using spin-polarized calculations. A comparison with non-spin-polarized (spin-unpolarized) calculations will be discussed in the next section. For all the pure 3d metal substrates considered, stable molecular adsorption configuration (i.e., $y = 4$ in $BH_y^* + (4 - y)H^*$) was found (left panel of Fig. 2). We used this adsorption configuration of borohydride on all the pure 3d metals in the analysis of magnetic properties (next Section). For this molecular configuration, borohydride chemisorbs through the H-up orientation with boron above the fcc hollow site and hydrogen atoms residing at the top sites. The preference for the fcc hollow over the hcp hollow site is very small (around 0.02 eV). This means that the presence (or absence) of atoms just below the hcp (or fcc) hollow site does not significantly affect the adsorption energetics. This supports the previous findings wherein a small preference between the fcc and hcp hollow sites were found for 4d and 5d transition metals [9]. The B-H bond lengths of borohydride for this molecular configuration on Cr, Mn, Fe, Co, and Ni are 1.31, 1.33, 1.37, 1.33, and 1.33 Å, respectively, as shown in Table 1. This falls within the B-H bond lengths (1.25–1.49 Å) reported in the literature for a molecularly adsorbed borohydride [9]. Our previous works have shown that this borohydride molecular configuration on fcc (111) surface of the metal substrate is characterized by the hybridization of the metal- d_{zz} state with BH_4 -sp states [6,10].

Stable dissociated adsorption structures for borohydride were also found. For the case of Mn and Fe surfaces, the adsorption at the bridge site (i.e., B atom on top of the bridge site) produces the $y = 2$ (in $BH_y^* + (4 - y)H^*$) configuration (middle panel in Fig. 2). This adsorption structure is 0.11 and 0.02 eV lower in energy than the molecularly adsorbed borohydride configuration ($y = 4$) at the hollow site of Mn and Fe, respectively. This structure was not found to be stable neither on the 4d and 5d metals previously studied nor on the other metals presented in this paper [9]. The dissociated hydrogen atoms reside on the neighboring hollow sites with B-H distances ranging from 2.18 to 2.28 Å. BH_2^* forms a bent structure on the plane perpendicular to the surface with inner angle equal to 102° for both Mn and Fe. Thus, there exists a borohydride chemisorption situation where $2H^*$ is formed rather

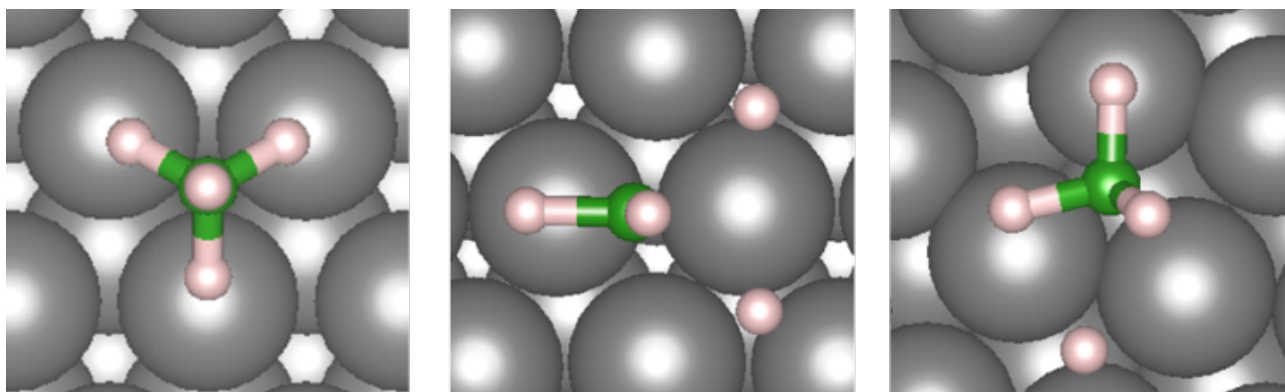


Fig. 2. The adsorption configurations of borohydride in the form of $BH_y^* + (4 - y)H^*$: molecular structure $y = 4$ (left); dissociated structure $y = 2$ (middle); dissociated structure $y = 3$ (right).

than the more commonly reported $3H^*$ case, which was previously found for Ir, Pd, and Pt. For this $y = 2$ ($BH_2^* + 2H^*$) configuration, our previous work has revealed the importance of the competing d_{zz} and $d_{xz,yz}$ interactions of the metal aimed at H and B of borohydride which results in an enhanced elongation of the two B-H bonds [30]. This interaction upon borohydride adsorption at the bridge site is enhanced by the closer distance of the adsorbed molecule on Mn and Fe compared to other metals considered. On the other hand, for the case of Cr surface, borohydride adsorption results in the $y = 1$ ($BH_3^* + H^*$) configuration as shown in the right panel of Fig. 2. The dissociated H atom is at 2.28Å distance from B while the B-H bond lengths for BH_3^* are within 1.20-1.33Å. This structure is 0.16 eV lower in energy than the molecularly adsorbed borohydride on the hollow site which was discussed earlier. We note a complex lateral relaxation of the top two layers of the Cr slab to accommodate this dissociated structure of borohydride.

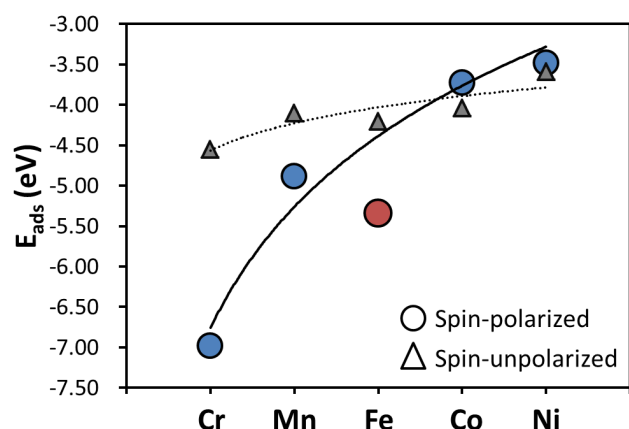


Fig. 3. The adsorption energy E_{ads} of borohydride on Cr, Mn, Fe, Co, and Ni. Circular and triangular data points denote the E_{ads} for spin-polarized and spin-unpolarized calculations, respectively. Trend lines (solid and dashed lines for spin-polarized and spin-unpolarized calculations, respectively) shown are generated by logarithmic curve fitting.

The calculated adsorption energy of a molecularly adsorbed borohydride on the surface for both spin-polarized and spin-unpolarized calculations is shown in Fig. 3. In this figure, circular and triangular data points denote the adsorption energies for the spin-polarized and spin-unpolarized calculations respectively, with trend lines generated by logarithmic curve fitting. Borohydride adsorption energy is strongest for Cr, followed by Fe, Mn, Co, and Ni in decreasing order of magnitude, for both spin-polarized and spin-unpolarized calculations. This general trend of decreasing adsorption energy from as we traverse the periodic table from left to right follows the well-established concept on the reactivity of metals [31]. Here, the tendency of adsorption energies to decrease from Cr to Ni can be explained by the interaction of sp band of the adsorbate with the metal d band which results in the formation of bonding and antibonding states with respect to adsorption. The overall energetics depends on the extent of filling of the antibonding state with respect to the Fermi energy. This derived sp-d antibonding state follows the position of the metal d band. Moving from Cr to Ni, the d band moves further below the Fermi energy. Thus, the extent of filling of the antibonding state from Cr to Cu increases which contributes to a repulsive interaction. It can be noticed from Fig. 3 that the adsorption energies from the spin-polarized calculation are “overbinding” with respect to the results from spin-unpolarized calculation for Cr, Mn, and Fe while “underbinding” for Co and Ni. For these metals, Table 1 shows that the B-H bond lengths of borohydride have not changed significantly. Thus, spin-polarization has a

major effect on the adsorption energy but has very little effect on the adsorption geometry of the adsorbate and relative energies of adsorbates on different substrates.

Table 1. Change in the fractional d band filling Δn_d , change in the magnetic moment of the three atoms bonded to borohydride ΔM , and B-H bond lengths.

Metal	Δn_d		ΔM (μ_B)	B-H bond (Å)	
	Spin-up	Spin-down		Spin-polarized	Spin-unpolarized
Cr	-0.01	0.01	0.942	1.31	1.31
Mn	-0.12	0.14	0.632	1.33	1.32
Fe	-0.26	0.27	3.78	1.37	1.35
Co	-0.04	0.03	0.924	1.33	1.38
Ni	-0.03	0.10	0.588	1.33	1.35

Interestingly, Fe has a large deviation from the trend (solid trend line in Fig. 3) of decreasing adsorption energies from Cr to Ni (as shown by the red data point in Fig. 3). This can be explained by the magnetic properties of Fe. For all these metals considered, the adsorption of borohydride results in the change of the fractional d band filling, n_d projected on the surface metal atom. Here, n_d is defined as:

$$n_d = \frac{\int_{-}^{E_F} \rho_d(E) dE}{\int_{-}^{+} \rho_d(E) dE} \quad (1)$$

where E_F is the Fermi level and $\rho_d(E)$ is the d band density of states. Note that the numerator and denominator were evaluated within the occupied states and whole d band, respectively. The reduction of the spin-up and the increase of the spin-down fractional d band filling, respectively, causes the forward shifting of the spin-up and backward shifting of the spin-down components of the d band before and after adsorption as shown schematically in Fig. 4. This phenomenon is accompanied by the change of the total magnetic moment for the *three* metal atoms directly bonded to borohydride. A dramatic change in the magnitude of the magnetic moment (ΔM in Table 1) is seen for Fe (3.78 μ_B), compared to relatively small changes for the other metals (Cr: 0.942 μ_B , Mn: 0.632 μ_B , Co: 0.924 μ_B , Ni: 0.588 μ_B). This finding is supported by the largest change in the spin-up and spin-down fractional d band filling, Δn_d , of Fe compared to other metals before and after the adsorption (Table 1). Thus, the large asymmetric shift of the Fe d band has a stabilizing effect on the adsorption of borohydride. The changes in the fractional d band filling occupancy $\Delta n_d = n_{d,adsorbed} - n_{d,clean}$ are reported in Table 1. Here, positive and negative values correspond to the backward and forward shifting of the d band respectively, illustrated in Fig. 4.

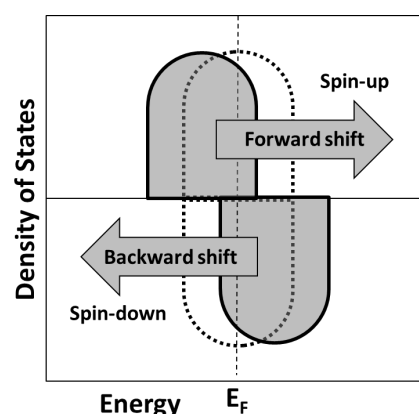


Fig. 4. A schematic diagram of the shifting of spin-up and spin-down components of the metal d band before (solid line) and after (dashed line) the adsorption of borohydride.

Borohydride on Au-3d metal alloys

Au-3d metal alloys were modeled as Au_3M ($M = Cr, Mn, Fe, Co, Ni$) with the $L1_2$ structure. Such alloys have been successfully synthesized in the laboratory and examined using a variety of experimental techniques, such as XRD and TEM [32-36]. Similar to the case of pure 3d transition metals, the (111) facet of the Au_3M metal alloys was used to rule out the structural differences between different surfaces and to extract meaningful trends in the properties as a function of the substrate identity. The calculated lattice constants are reported in Table 2, which are in excellent agreement with experiments [34].

Table 2. Lattice constants, borohydride adsorption energy, change in the fractional d band filling Δn_d , change in the magnetic moment of M ($M = Cr, Fe, Mn, Co, Ni$) atom bonded to borohydride ΔM , and B-H bond lengths.

Metal	Lattice constants (Å)	E_{ads} (eV)	Δn_d		ΔM (μ_B)	B-H bond (Å)
			Spin-up	Spin-down		
Au ₃ Cr	4.07	-2.31	-0.06	0.05	0.507	1.28
Au ₃ Mn	4.05	-2.19	-0.01	0.03	0.169	1.26
Au ₃ Fe	4.04	-2.34	-0.02	0.01	0.196	1.28
Au ₃ Co	4.03	-2.41	-0.15	0.17	1.612	1.36
Au ₃ Ni	4.03	-2.16	-0.06	0.04	0.217	1.32

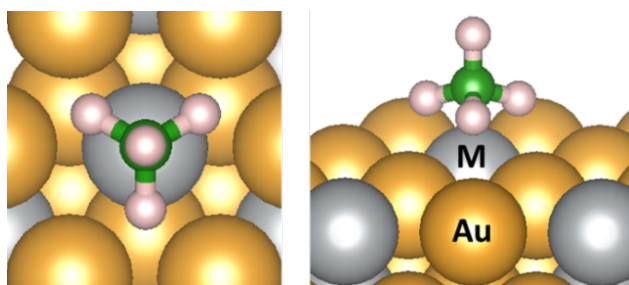


Fig. 5. Adsorption structure of borohydride on Au-3d alloys. The atom labelled M is a 3d atom.

For these Au-3d alloys, borohydride tends to “seek” the alloying metal by adsorbing on the surface with B on top of the alloying metal M, and H atoms on the hollow sites as shown in Fig. 5. Similar to the borohydride molecular structure on pure 3d metals, the B-H bond lengths of borohydride on all these alloys fall within the previously set B-H bond lengths (1.26-1.49 Å) for the case of molecularly adsorbed borohydride (Table 2). For $Au_3M(111)$ with $M = Cr, Mn$ and Fe , the B-H bond lengths are almost the same as that for pure Au (1.26-1.28 Å) [6]. While for $M = Co$ and Ni , the B-H bond lengths are more elongated (1.36 and 1.32 Å respectively). To understand this, we analyzed the DOS projected on the surface alloying atom M for the clean and adsorbed systems. For all these alloys, the components of the d band that protrude out of the surface (d_{zz}, d_{xz}, d_{yz}) interact with borohydride. However, the shift and formation of new peaks for “surface-parallel” components of the d band (d_{xy} and $d_{x^2-y^2}$) are noted only for $M = Co$ and Ni alloys. We show this in Figure 6 using the Local-DOS of Fe (representing Au_3M alloys with $M = Cr, Mn$ and Fe) and Co (representing Au_3M alloys with $M = Co$ and Ni) atoms projected on d_{xy} and $d_{x^2-y^2}$ states. Thus, the interaction of borohydride with surface-parallel components of the d band leads to further elongation of the borohydride B-H bonds for $M = Co$ and Ni cases. It can be argued from Figure 6 that the magnetic moment of Co has almost diminished upon borohydride adsorption (from 1.905 μ_B to 0.293 μ_B). However, this large decrease in the magnetic moment of Co is not

observed for Ni (from 0.328 μ_B to 0.111 μ_B). Thus, the demagnetization of the substrate can be ruled out as the cause of the shifting of DOS peaks for d_{xy} and $d_{x^2-y^2}$ components of the d band of Co and Ni.

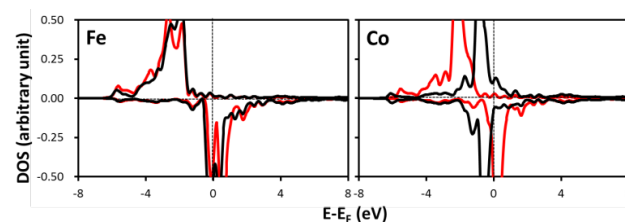


Fig. 6. Density of states projected on components of the d band of Fe (to represent the $M = Cr, Mn$ and Fe cases) and Co (to represent the $M = Co$ and Ni case). The red and black curves correspond to the clean surface and the surface with adsorbed borohydride, respectively. The positive and negative values of density of states correspond to spin-up and spin-down states, respectively.

The adsorption energy of borohydride on these alloys is presented in Table 2. The difference between the weakest (for Au_3Ni) and strongest (for Au_3Co) adsorption energies is only 0.25 eV which is relatively very small compared to the difference in adsorption energies (3.50 eV) for the pure 3d metals. The strongest adsorption energy is found for Au_3Co . For these alloy systems, the earlier discussed stabilizing effect of the substrate demagnetization on borohydride adsorption was also found. In Table 2, we show the change in the fractional d band filling evaluated for spin-up and spin-down components of the d band of the alloying atom M which bonds directly with borohydride. Similar to the case of pure 3d metals discussed earlier, the forward shifting of the spin-up and backward shifting of the spin-down components of the d band are observed. The largest asymmetric shift of spin-up and spin-down components are seen for Au_3Co which corresponds to the largest change in the magnetic moment of Co as shown in Table 2. Such large demagnetization of Co corresponds to the largest magnitude of borohydride adsorption energy on Au_3Co .

CONCLUSION

Using first principles density functional theory based calculations, we have shown that the adsorption of borohydride induces the demagnetization of the substrate atoms that directly bind with it. This phenomenon is observed for both pure and alloyed magnetic substrates. The inclusion of the spin-polarization in the calculation affects the adsorption energy of borohydride but not its adsorption structure and relative energies on different substrates. Among the pure 3d metals considered ($Cr, Mn, Fe, Co,$ and Ni), the forward shifting of the spin-up and conversely the backward shifting of the spin-down components of the metal d band, before and after the adsorption of borohydride, was most pronounced for the case of Fe substrate. This had a stabilizing effect on the adsorption of borohydride. Similar demagnetization is found for Au-3d metal alloys.

ACKNOWLEDGEMENT

Some of the calculations were done using the computer facilities of Cyber Media Center (Osaka University), ISSP Super Computer Center (University of Tokyo), and Large Scale Simulation Program KEK No.T10-12 of High Energy Accelerator Research Organization, Kyoto Supercomputer and High Performance Computing Cluster, Fukui (HPCCF). M.C. Ecaño would like to thank the Special Coordination Funds for the Promotion of Science and Technology of the Ministry of Education, Culture and Sports (MEXT) through the Tenure

Track Program for Innovative Research, University of Fukui for research funds. A.A.B. Padama acknowledges and is grateful to the University of the Philippines Balik PhD Research Grant (BPhD 2015-07). The authors acknowledge Prof. Elod Gyenge and Andrew Yu-Sheng Wang of the Department of Chemical and Biological Engineering of the University of British Columbia, Vancouver, Canada for fruitful collaborations through the years.

REFERENCES

- [1] Matsunaka D, Kasai H, Dino WA, Nakanishi H. Magnetic properties in the high-temperature cuprate superconductors with nonmagnetic impurities. *Phys. Rev. B* 2003; 68:054503-054507.
- [2] Minamitani E, Dino WA, Nakanishi H, Kasai H. Effect of antiferromagnetic RKKY interaction and magnetic field in a two-impurity Kondo system. *Phys. Rev. B* 2010; 82:153203-153206.
- [3] Hoa NTM, Minamitani E, Dino WA, Cong BT, Kasai H. Effect of RKKY interaction on the system of two magnetic atoms on a metal surface at finite temperatures. *J. Phys. Soc. Jpn.* 2010; 79:074702-074705.
- [4] Spisak D, Hafner J. Adsorbate-induced demagnetization and restructuring of ultrathin magnetic films: CO chemisorbed on γ -Fe/Cu(110). *Phys. Rev. B* 2001; 64:094418-094429.
- [5] Jerkins SJ, Ge Q, King DA. Covalent origin of adsorbate-induced demagnetization at ferromagnetic surfaces. *Phys. Rev. B* 2001; 64:012413-012416.
- [6] Arevalo RL, Escano MCS, Wang AYS, Kasai H. Structure and stability of borohydride on Au(111) and $\text{Au}_3\text{M}(111)$ (M = Cr, Mn, Fe, Co, Ni) surfaces. *Dalton Trans* 2012; 42:770-775.
- [7] Arevalo RL, Escano MCS, Gyenge E, Kasai H. A theoretical study of the structure and stability of borohydride on 3d transition metals. *Surf. Sci.* 2012; 606:1954-1959.
- [8] Arevalo RL, Escano MCS, Kasai H. Computational mechanistic study of borohydride electrochemical oxidation on $\text{Au}_3\text{Ni}(111)$. *J. Phys. Chem. C* 2013; 117:3818-3825.
- [9] Escano MCS, Gyenge E, Arevalo RL, Kasai H. Reactivity descriptors for borohydride interaction with metal surfaces. *J. Phys. Chem. C* 2011; 115:19883-19889.
- [10] Arevalo RL, Escano MCS, Kasai H. Mechanistic Insight into the Au-3d Metal Alloy-Catalyzed Borohydride Electro-Oxidation: From Electronic Properties to Thermodynamics. *ACS Catal* 2013; 3:3031-3040.
- [11] Kunisada Y, Kishi H, Dimas F, David M, Nakanishi H, Kasai H, Asari T, Hayashi S. Adsorption properties of BF_4^- anions on graphene. *Jpn. J. Appl. Phys.* 2010; 49:02BB04-02BB06.
- [12] Roques J, Anderson A, Murthi V, Mukerjee S. Potential shift for OH(ads) formation on the Pt skin on $\text{Pt}_3\text{Co}(111)$ electrodes in acid: theory and experiment. *J. Electrochem. Soc.* 2005; 151:E193-E199.
- [13] Xin H, Linic S. Communications: Exceptions to the d-band model of chemisorption on metal surfaces: The dominant role of repulsion between adsorbate states and metal d-states. *J. Chem. Phys.* 2010; 132:221101-221104.
- [14] Shen J, Gai Z, Kirschner J. Growth and magnetism of metallic thin films and multilayers by pulsed-laser deposition. *Surf. Sci. Rep.* 2004; 52:163-218.
- [15] Wang HH, Guo GY. Gradient-corrected density functional calculation of structural and magnetic properties of BCC, FCC and HCP Cr. *J. Magn. Magn. Mater.* 2000; 209:98-99.
- [16] Mehl MJ, Papaconstantopoulos DA. Applications of tight-binding total-energy method for transition and noble metals: Elastic constants, vacancies, and surfaces of monatomic metals. *Phys. Rev. B* 1996; 54:4519-4530.
- [17] Zhang M, Pan F, Liu BX. Magnetic properties of fcc iron in Fe - Pt nano-scale multilayers. *J. Phys.: Condens. Matter* 1997; 9:7623-7630.
- [18] Schastlivtsev VM, Ustinov VV, et al. Nickel alloy substrates with a sharp cube texture for high-Tc superconducting tapes. *Doklady Akademii Nauk* 2003; 395:167-170.
- [19] Kresse G, Furthmuller J. Efficiency of ab-initio total energy calculations for metals and semiconductors using a plane-wave basis set. *Comput. Mater. Sci.* 1996; 6:15-50.
- [20] Kresse G, Furthmuller J. Efficient iterative schemes for ab initio total-energy calculations using a plane-wave basis set. *Phys. Rev. B* 1996; 54:11169-11186.
- [21] Kresse G, Hafner J. Ab initio molecular dynamics for liquid metals. *Phys. Rev. B* 1993; 47:558-561.
- [22] Kresse G, Hafner J. Ab initio molecular-dynamics simulation of the liquid-metal-amorphous-semiconductor transition in germanium. *Phys. Rev. B* 1994; 49:14251-14269.
- [23] Kresse G, Joubert J. From ultrasoft pseudopotentials to the projector augmented-wave method. *Phys. Rev. B* 1999; 59:1758-1775.
- [24] Blochl PE. Projector augmented-wave method. *Phys. Rev. B* 1994; 50:17953-17979.
- [25] Perdew J, Burke K, Ernzerhof M. Generalized gradient approximation made simple. *Phys. Rev. Lett.* 1997; 78:1396.
- [26] Perdew J, Burke K, Ernzerhof M. Generalized gradient approximation made simple. *Phys. Rev. Lett.* 1996; 77:3865-3868.
- [27] Monkhorst HJ, Pack JD. Special points for Brillouin-zone integration in metals. *Phys. Rev. B* 1976; 13:5188-5192.
- [28] Methfessel M, Paxton A. High-precision sampling for Brillouin-zone integration in metals. *Phys. Rev. B* 1989; 40:3616-3621.
- [29] Stich I, Car R, Parrinello M, Baroni S. Conjugate gradient minimization of the energy functional: A new method for electronic structure calculation. *Phys. Rev. B* 1989; 39:4997-5004.
- [30] Arevalo RL, Escano MCS, Kasai H. First principles study on the adsorption and dehydrogenation of borohydride on Mn (111). *e-J. Surf. Sci. Nanotech.* 2011; 9:257-264.
- [31] Hammer B, Norskov JK. Why gold is the noblest of all the metals. *Nature* 1995; 376:238-241.
- [32] Vasquez Y, Luo Z, Schaak RE. Low-temperature solution synthesis of the non-equilibrium ordered intermetallic compounds Au_3Fe , Au_3Co , and Au_3Ni as nanocrystals. *J. Am. Chem. Soc.* 2008; 130:11866-11867.
- [33] Yamamoto K. Electron diffraction study on thin films around Au_3Mn . *Phys. Status. Solidi* 1980; 59:767-777.
- [34] Dutkiewicz J, Thomas G. High resolution study of ordering reactions in gold-chromium alloys. *Metall. Trans. A* 1975; 6A:1919-1928.
- [35] Sato H, Toth RS, Honjo G. Long period stacking order in close packed structures of metals. *J. Phys. Chem. Solids* 1967; 28:137-160.
- [36] Sato H, Toth RS, Shirane G, Cox DE. Long period modulation of stacking order in Au_3Mn . *J. Phys. Chem. Solids* 1966; 27:413-422.